How Long Can the Hubble Space Telescope Operate Reliably? – A Total Dose Perspective

M.A. Xapsos, C. Stauffer, T. Jordan, C. Poivey, D.N. Haskins, G. Lum, A.M. Pergosky, D.C. Smith, and K.A. LaBel

***Abstract*— The Hubble Space Telescope has been at the forefront of discoveries in the field of astronomy for more than 20 years. It was the first telescope designed to be serviced in space and the last such servicing mission occurred in May 2009. The question of how much longer this valuable resource can continue to return science data remains. In this paper a detailed analysis of the total dose exposure of electronic parts at the box level is performed using solid angle sectoring/3-dimensional ray trace and Monte Carlo radiation transport simulations. Results are related to parts that have been proposed as possible total dose concerns. The spacecraft subsystem that appears to be at the greatest risk for total dose failure is identified. This is discussed with perspective on the overall lifetime of the spacecraft.**

***Index Terms*—Hubble Space Telescope, radiation shielding, radiation transport, total ionizing dose, Van Allen belts**

I. Introduction

The Hubble Space Telescope (HST) was deployed from the space shuttle Discovery on April 25, 1990 into a low Earth orbit (LEO) with an approximate altitude of 569 km and inclination of 28.5 degrees. Although its primary 2.4 meter diameter mirror is not large in comparison to ground-based telescopes the advantages of being in orbit have contributed to its extraordinary scientific success. Being outside Earth's atmosphere avoids atmospheric distortions and almost all background light so that very high resolution images can be taken. In addition it allows HST to view portions of the ultraviolet and infrared spectra not observable with Earth-based telescopes.

HST's observations and discoveries have ranged from those in our own solar system to nearly the edge of the universe. They have given views of the universe within a few hundred million years of the Big Bang and helped establish its age of 13.7 billion years. Possibly the most profound conclusion has been drawn from observation of light emitted by a certain category of supernova explosions, which is that the expansion of the universe is not slowing due to gravity but accelerating. This is attributed to dark energy, an apparently dilute entity spread over all space that is significant on a cosmological scale. One of the deepest images of the universe in optical light is shown in Fig. 1. HST helped establish how galaxies are formed and evolve from the generally smaller and irregular galaxies billions of years ago to the larger and more structured galaxies of recent times such as spiral and elliptical galaxies.

Within our solar system HST images of the fragmented comet Shoemaker-Levy 9 colliding with Jupiter helped raise public awareness about potential comet and asteroid collisions with Earth. Many more significant observations and discoveries by HST exist that are much too numerous to mention. Reference [1] provides an excellent overview.

II. Servicing Missions

HST was the first telescope designed to be serviced in space. The servicing missions are the primary reason that it has functioned at such a high level for a long period of time [2]. Following its deployment in April 1990 a much publicized spherical aberration was discovered in the primary mirror in June of that year. Servicing Mission 1 (SM1), which occurred in December 1993, was used to correct the mirror's flaw by installing corrective optics. It was also used to replace the wide field planetary camera with an improved one and for planned maintenance. Servicing Mission 2 (SM2) occurred in February 1997. It featured the installation

Manuscript submitted July 10, 2014. Revised September 11, 2014. This work is supported by the Hubble Space Telescope Program.

M.A. Xapsos is with NASA Goddard Space Flight Center, Greenbelt, MD, 20771 USA (e-mail: Michael.A.Xapsos@nasa.gov).

C. Stauffer is with AS&D, Inc., Greenbelt, MD, USA.

T. Jordan is with EMP Consultants, Gaithersburg, MD, USA

C. Poivey is with ESA-ESTEC, Noordwijk, The Netherlands

D.N. Haskins is with NASA Goddard Space Flight Center, Greenbelt, MD, USA

G. Lum is with Lockheed Martin Space Systems Company, Sunnyvale, CA, USA

A.M. Pergosky is with Lockheed Martin Information System and Global Services, Greenbelt, MD, USA

D.C. Smith is with Lockheed Martin Space Systems Company, Greenbelt, MD, USA

K.A. LaBel is with NASA Goddard Space Flight Center, Greenbelt, MD, USA

Fig. 1. HST image of the universe looking back in time, from http://hubblesite.org. Credit: NASA, ESA, S. Beckwith (Space Telescope Science Institute), Hubble Ultra-Deep Field team.

of two new instruments that gave HST new spectroscopic capabilities and the ability to view much more distant objects in the universe at near-infrared wavelengths. A number of other hardware items were installed or replaced for spacecraft maintenance. Servicing Mission 3 (SM3) was initially viewed as preventative maintenance but in 1999 a third gyroscope failure occurred leaving only 3 functioning gyroscopes onboard, the number required for the Pointing Control System at that time. NASA addressed this by splitting SM3 into two parts, SM3A and SM3B. In November 1999 a fourth gyroscope failed, forcing HST into "safe mode" and science operations stopped. This lasted about 6 weeks until SM3A occurred in December 1999. SM3A replaced all 6 gyroscopes and made a number of other substantial improvements that included a new main computer, new solid state recorder and an enhanced fine guidance sensor. SM3B occurred in March 2002 and saw the installation of a new instrument, the Advanced Camera for Surveys (ACS). At this point all of the original instruments had been replaced. The Near Infrared Camera and Multi-Object Spectrometer (NICMOS) was revived by the installation of a new cooling system. Spacecraft power was addressed with installation of a new set of solar arrays and a new power control unit. The new solar arrays, in addition to being more efficient, were also smaller in size resulting in less atmospheric drag. Servicing Mission 4 (SM4), the final HST servicing mission, was originally planned to occur in 2005. However, things took several dramatic turns following the Columbia disaster in 2003 in which the shuttle disintegrated upon re-entry to the atmosphere. In a controversial decision NASA cancelled SM4, citing safety reasons. Following protests from the scientific community, the public and questions from the United States Congress, Goddard Space Flight Center (GSFC) was tasked with investigating the possibility of a robotic service mission to HST. With the subsequent appointment of a new NASA Administrator the shuttle servicing mission was re-evaluated and SM4 was scheduled for October 2008. In the prior month, however, the primary science instrument Command & Data Handling channel failed, leaving the back-up as a single point failure to science operations. SM4 was re-scheduled one last time for May 2009 to allow a replacement module to be installed in addition to other planned activities. This included considerable improvement of instrumentation with the installation of two new instruments – the Cosmic Origins Spectrograph (COS) and Wide Field Camera 3 (WFC3), and the repair of 2 instruments – the Space Telescope Imaging Spectrograph (STIS) and the ACS. All 6 batteries and all 6 gyroscopes were replaced, and a refurbished Fine Guidance Sensor (FGS) was installed in addition to other activities.

The James Webb Space Telescope (JWST), generally regarded as the successor to HST, will be launched no sooner than 2018. For scientific reasons it is preferable that the two telescopes operate simultaneously for at least a year or two. One of the issues that has come to the forefront in this regard is the total ionizing dose (TID) exposure of microelectronic components in HST. A 2005 report issued by the National Academy of Sciences found that "Adverse radiation effects after 2010 are more likely, with an increasing risk of avionics component failures if science operations are extended until 2014" [3]. The purpose of this paper is to evaluate the possibility of TID failures in HST until JWST is commissioned and beyond. The analysis is done in greater detail than has been considered previously and with a newer and more appropriate model for the radiation environment. These new results are useful for HST's contingency planning and life extension initiatives. Other significant factors along these lines not discussed here include battery, gyroscope, fine guidance sensor and instrument lifetimes; avionics system reliability; and orbital decay [3,4].

III. Methods

Due to the longevity of HST the main radiation concern at this point is a hard failure due to TID or displacement damage that could bring science operations to a halt. The potential for TID failures in HST has been investigated on several occasions internally at GSFC with limited detail about shielding. Consequently worst case assumptions were typically made in these analyses [5-7]. In an effort to provide a more robust analysis an extensive review of the HST mechanical design was undertaken, particularly the subsystem and instrument dimensions and wall thicknesses, masses and placement within the spacecraft.

The Numerical Optimizations, Visualizations, and Integrations on Computer Aided Design (CAD)/Constructive Solid Geometry (CSG) Edifices (NOVICE) code [8] was used for analysis by solid angle sectoring/3-dimensional ray trace and Monte Carlo radiation transport. This code has two main advantages. First it interfaces with CAD models, allowing complex shielding geometries such as spacecraft to be analyzed. Second, it runs in an adjoint mode, as opposed to a

forward mode, which greatly increases the calculation efficiency. A detailed CAD model of the HST spacecraft (not including the subsystems and instruments) was obtained from Lockheed Martin and converted to the NOVICE radiation model shown in Fig.2. Layout and box locations were provided and were used to cross-check information in the mechanical design. Instruments are generally placed toward the bottom (left side of Fig.2) of the spacecraft behind the primary mirror. Subsystems are generally more toward the periphery in bay regions for the optical telescope assembly and support systems. The interiors of the spacecraft top door, bottom and walls were converted to honeycomb material to match their known composition. The total mass of each box and instrument is accurately known but the internal mass distribution within each unit was not readily available for this analysis. It was therefore assumed that except for electronics boards the interior mass was uniformly distributed within each unit and was given a density such that the total mass equaled the known mass of the unit. Electronics boards were placed in units based on the position of connectors shown in mechanical drawings. Two 3 x 3 arrays of virtual radiation dose detectors were placed on the top and bottom sides of each board to evaluate the dose variation. The reported doses are the mean, maximum and minimum values seen in the virtual detectors for each unit. The total mass accounted for in these simulations was 96% of the actual HST mass of 12,218 kg. This seems quite reasonable considering the simulation does not include items such as cabling.

The five servicing missions add a degree of complexity to the TID analysis. In some cases components are exposed to TID from launch to the end of mission. In other cases they are exposed from a servicing mission to mission end or even from one servicing to a subsequent servicing. Thus, similar to Poivey [6] a procedure was implemented to track the start and end dates of TID exposure of all components.

Next the choice of radiation environment models is considered. At the electronics shielding levels of HST, TID is mainly due to trapped protons with a smaller contribution from trapped electrons. The dose due to solar events in this low Earth, low inclination orbit is very small by comparison because of geomagnetic shielding. The trapped proton flux in LEO is anisotropic. However, HST has been maneuvered many times to focus on objects and regions of space in varying directions. The proton flux for the purpose of TID calculations is therefore assumed to be isotropically incident. The long-time standard Aerospace Proton-8 (AP-8) model [9] for trapped protons is now out of date and known to have shortcomings [10]. Consequently there have been a number of notable efforts to develop new trapped proton models [11-14]. In principle the environment for HST from its 1990 launch to the present is known so it is preferable to use a trapped proton model that is calibrated to environmental parameters during these times. This should include a description of solar cycle dependence because the HST servicing missions occurred during different phases of the solar cycle. The only trapped proton model that satisfies these criteria is the Boeing Trapped Proton Model-1 (TPM-1) [11], a model based largely on the long-term Television Infrared

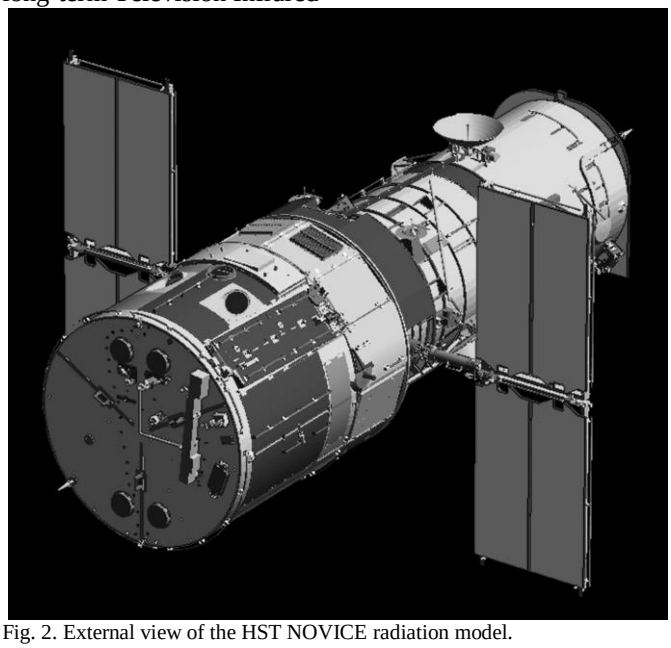

Fig. 2. External view of the HST NOVICE radiation model.

Observation Satellites (TIROS) data for LEO. The solar cycle dependence is obtained from a solar activity scaling factor for a given time and location determined from the 10.7 cm solar flux, F10.7. This accounts for the modulation of LEO proton fluxes by the influence of solar activity on the Earth's atmosphere. Further TPM-1 is in good agreement with the data of Ginet et al., particularly at the altitudes of HST [15]. This model also allows proton flux predictions for future dates with the incorporation of forecast F10.7 values, which are fairly well known out to the year 2020 [16]. The model comes with F10.7 data ranging from 1960 to August 2001. For the current simulations these were updated by inserting the smoothed data from January 2000 to August 2013 and the consensus values of the Solar Cycle 24 Prediction Panel from September 2013 through December 2019, obtained from reference [16]. The 81.3 MeV differential proton flux calculated from this model is shown in Fig.3 over the time period from 1990 to 2020. A shortcoming of this model is that the proton energies are limited in range from 1.5 to 81.3 MeV. The new AP-9 model, version 1.2, was therefore used to extrapolate the energy spectra out to 2 GeV. This was done by normalizing each energy spectrum to the average fluence of the two models at 81.3 MeV. The resulting average value is in close agreement with trapped proton data measured by the Solar Anomalous and Magnetospheric Particle Explorer (SAMPEX) instrumentation [12]. The utility of AP-9 for this study is limited to this because it does not contain an explicit solar cycle dependence.

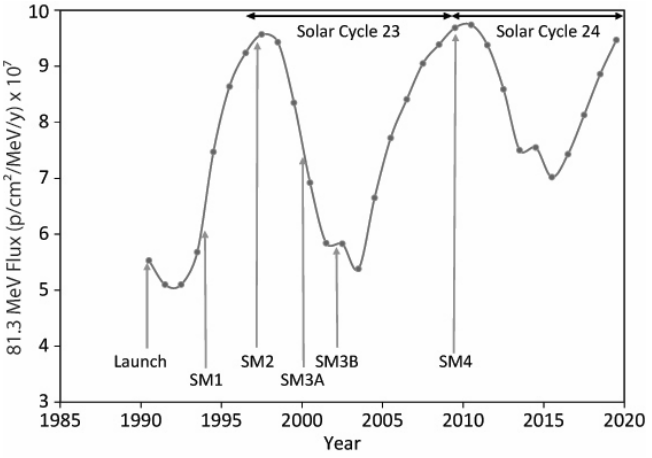

Fig. 3. Trapped proton fluxes for the HST orbit from launch to the year 2020 calculated with the Boeing TPM-1 [11] using updated input. Also shown are the launch date and dates of the 5 servicing missions. Note the proton fluxes are approximately anti-correlated to solar cycle activity.

The choice of a trapped electron model has little influence on the final results because the TID due to trapped electrons is substantially less than that due to trapped protons. The Aerospace Electron-8 (AE8) model [17] was chosen on the basis that it contains approximate solar cycle dependence.

IV. Results

Fig. 4 shows results for 6 TID vs. shielding depth curves from launch and each servicing mission to the start of calendar year 2020. The curves were calculated using the methods described above. In order to obtain an initial assessment of the situation the shielding geometry was first assumed to be a solid aluminum sphere. The sharp fall-off of the curves for shielding thickness < 25 mils is due to the relative ease at which electrons and protons with energy less than about 10 MeV are attenuated by shielding. This result verifies that the dose due to high energy protons is the main contribution for shielding relevant for the spacecraft electronics.

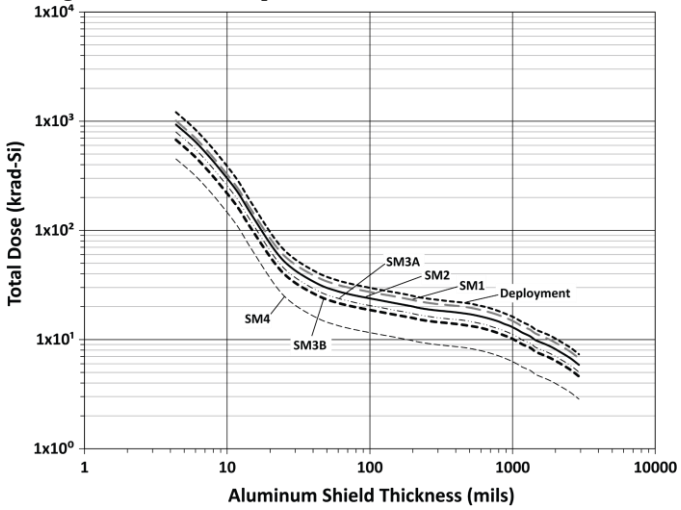

Fig. 4. TID curves for the HST environment assuming a shielding geometry of solid aluminum spheres. Results are shown to 1/1/2020 from 6 different starting times – deployment and the 5 servicing missions.

Fig. 5 shows the expected dose for each instrument and subsystem unit currently onboard HST using the model shown in Fig.2. Acronyms are defined in Appendix I. Calculations were done from the time the unit was inserted until 1/1/2020. The doses range from about 2.5 to 11 krad(Si). As described in section III the error bars represent the maximum and minimum dose values within each unit.

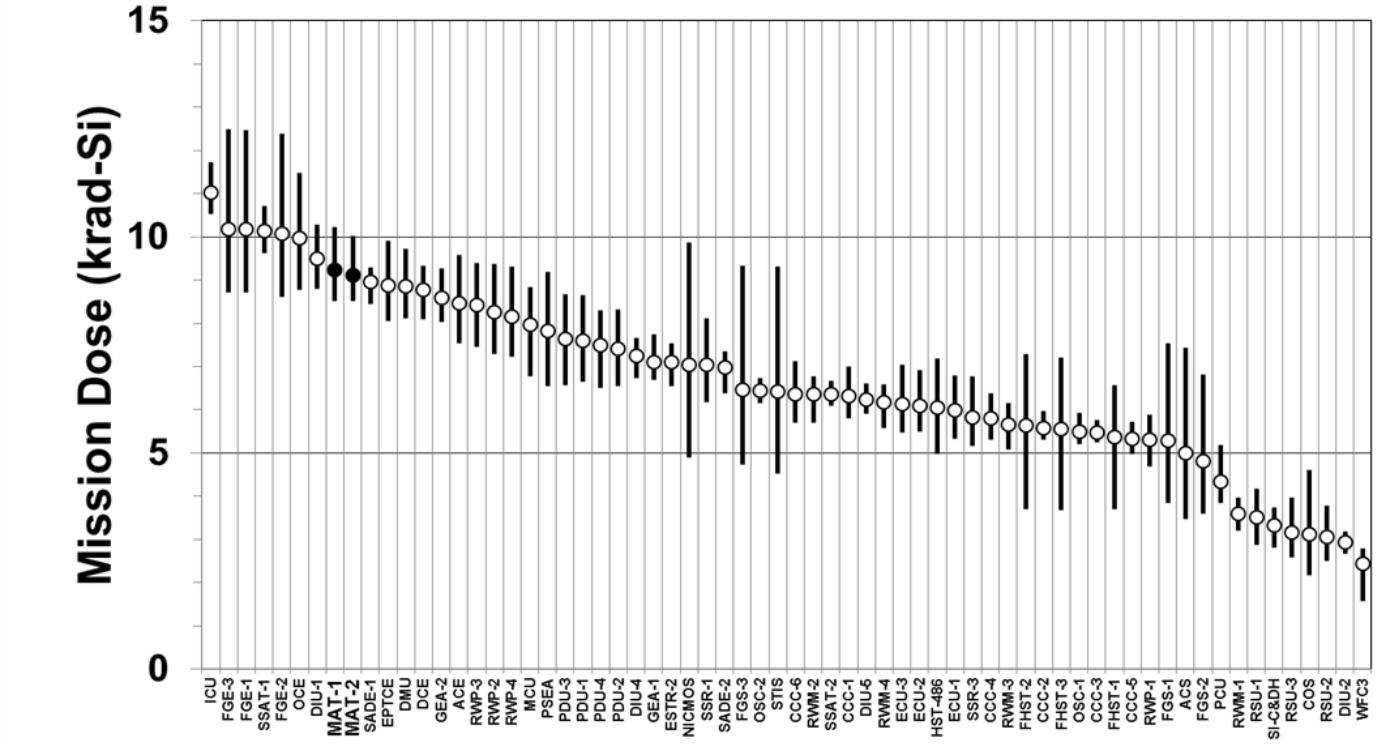

Fig. 5. Mission dose levels predicted from solid angle sectoring/3-dimensional ray trace and Monte Carlo calculations for 66 instrument and subsystem units currently onboard HST. The MAT-1 and MAT-2 units shown by solid points contain electronic parts identified as TID concerns. See Appendix I for the definition of acronyms.

The TID requirements for HST parts range from 5 to 15 krad(Si). However, conflicting reports exist as to how these numbers were derived. The HST Parts and Control Plan specifies this should depend on whether test data for parts are generic or flight lot specific. On the other hand a Lockheed Martin report specifies the requirement is 3 times the calculated solar minimum dose for a 5 year period where the dose is calculated inside specific areas of the spacecraft [18]. In any event both specifications produce a range of approximately 5 to 15 krad(Si). From the box level perspective shown in Fig.5 the exposure of the majority of units falls within the 5 to 15 krad(Si) dose requirement range, indicating potential problems. However, these are the minimal TID requirements for electronics and a review of a large number of parts showed that they were often selected to significantly exceed these requirements [18]. Examination of available parts lists showed many parts were procured to be TID hard to 100 krad(Si).

There are over 14,000 electronic parts procured for HST dating back to pre-launch so an exhaustive parts analysis is no longer realistic. Parts analyses have been done in the past that have identified key components as potential concerns. The most extensive of these, reference [18], grouped parts into families of technologies, ranging from the CD4000 series Complementary Metal Oxide Semiconductor (CMOS), the S series Schottky bipolar, the LS series low power Schottky bipolar and the L series low power bipolar. In addition there were the LM series bipolar linears. Within each family of technology an attempt was made to obtain radiation data and if the technology appeared to be fairly robust, i.e., tolerant to at least 50 krad(Si), spot checks of a few part types within a family were made. Attention was paid to bipolar parts in light of the fact that the Enhanced Low Dose Rate Sensitivity (ELDRS) effect was not discovered until after the launch of HST. Data were mainly obtained from the DoD Nuclear Information Analysis Center (DASIAC), which housed data going as far back as 1976 but is no longer available for use. These results are summarized in Appendix II. HST was initially developed in the 1980s when bipolar technologies were generally more advanced and TID hard than CMOS technology. As a result the parts listed turned out to be all CMOS. Inspection of the appendix indicates that the multiple access transponder (MAT) units are a concern going forward because they contain microprocessors, Random Access Memory (RAM) and Read Only Memory (ROM) with low TID hardness that has already been significantly exceeded beyond the uncertainty in the simulation. The build-up of dose in MAT-1 over the course of the mission and up to 2020 is shown in Fig.6 along with the TID exposure for each year. However, there are several factors that work in favor of the continued operation of these units. Annealing of the parts is not accounted for in the simulation and this is likely significant considering the length of time these parts have been in orbit. In addition the specified TID hardness could be conservative due to the test methodology chosen such as bias conditions and dose rates. Finally, the parts may still operate satisfactorily even if their parameters begin to go out of the manufacturers specifications. The latter appears to be the case

for the Field Programmable Gate Arrays (FPGAs) in the solid state recorders shown in Appendix II. These arrays develop increased leakage current in the 5 – 10 krad(Si) dose range but otherwise perform well out to 15 krad(Si) [19].

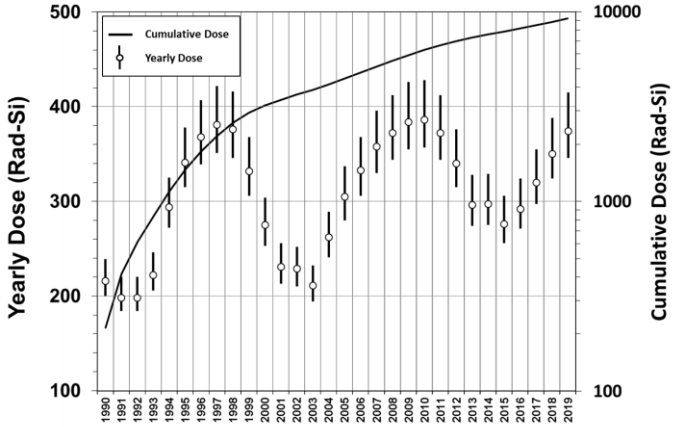

Fig. 6. Annual doses received by MAT-1 over the course of the HST mission and projected out to 2020 shown on the left-hand axis. The right hand axis is the corresponding cumulative dose.

It was reported that a radiation failure was believed to have occurred in a GaAs LED used in an optical encoder of a fine guidance sensor (FGS) [3]. The LED was characterized by a reduced light output over time and is no longer onboard HST. However, a thorough investigation of the flight lot LEDs at GSFC indicated the most likely cause of the failure was a degraded solder joint [20]. Our radiation simulations support this as well. If the LED failure was due to radiation it would be a result of displacement damage. The exposure of the failed unit was calculated using nonionizing energy loss [21] to determine equivalent fluences of 1 MeV neutrons and 10 MeV protons in GaAs. These results are shown in Table I for the failed unit, FGS-0, and three other units currently onboard HST. All LEDs are from the same flight lot. Since the performance of the other three LEDs has not deteriorated substantially in spite of their greater exposure our simulations are not consistent with a radiation failure of FGS-0.

TABLE I
Equivalent fluences of 1 MeV neutrons and 10 MeV protons for GaAs LEDs in all FGS units. The failed LED is listed as FGS-0.

FGS Unit	1 MeV n (cm^{-2})	10 MeV p (cm^{-2})
FGS-0	5.75×10^{10}	1.85×10^{10}
FGS-1	8.91×10^{10}	2.87×10^{10}
FGS-2	8.10×10^{10}	2.61×10^{10}
FGS-3	1.09×10^{11}	3.50×10^{10}

V. Conclusions

The Hubble Space Telescope has been in orbit for over 24 years. As a result of its longevity, potential total dose failures have become an important consideration for the mission's continuation. A complete TID analysis of HST has been performed at the box level and compared to electronic and photonic parts that are potential problems. From this analysis the biggest radiation concern is the performance of several parts in the transponder units although the parts analysis is not a complete one. Calculation of nonionizing dose exposure of FGS units indicated that LED degradation in optical encoders due to displacement damage should not limit their performance. The results of this analysis are beneficial to the HST Project in their contingency planning and prioritization of life extension initiatives.

Appendix I

Mean doses expected within units currently onboard HST at the start of calendar year 2020.

Acronym	Name	Time of Insertion	Dose (krad-Si)
ACE	Actuator Control Electronics	Launch	8.5
ACS	Advanced Camera for Surveys	SM3B	5.0
CCC-1	Charge Current Controller-1	Launch	6.3
CCC-2	Charge Current Controller-2	Launch	5.6
CCC-3	Charge Current Controller-3	Launch	5.5
CCC-4	Charge Current Controller-4	Launch	5.8
CCC-5	Charge Current Controller-5	Launch	5.3
CCC-6	Charge Current Controller-6	Launch	6.4
COS	Cosmic Origins Spectrograph	SM4	3.1
DCE	Deployment Control Electronics	Launch	8.8
DIU-1	Data Interface Unit-1	Launch	9.5
DIU-2	Data Interface Unit-2	SM2	2.9
DIU-4	Data Interface Unit-4	Launch	7.2
DIU-5	Data Interface Unit-5	Launch	6.2
DMU	Data Management Unit	Launch	8.9
ECU-1	Electronic Control Unit-1	SM1	6.0
ECU-2	Electronic Control Unit-2	Launch	6.1
ECU-3	Electronic Control Unit-3	SM1	6.1
EP/TCE	Electrical Power/Thermal Control Electronics	Launch	8.9
ESTR-2	Engineering Science Tape Recorder-2	SM2	7.1
FGE-1	Fine Guidance Electronics-1	Launch	10.2
FGE-2	Fine Guidance Electronics-2	Launch	10.1
FGE-3	Fine Guidance Electronics-3	Launch	10.2
FGS-1	Fine Guidance Sensor-1	SM2	5.3
FGS-2	Fine Guidance Sensor-2	Launch and SM4*	4.8
FGS-3	Fine Guidance Sensor-3	Launch	6.5
FHST-1	Fixed Head Star Tracker-1	Launch	5.4
FHST-2	Fixed Head Star Tracker-2	Launch	5.6
FHST-3	Fixed Head Star Tracker-3	Launch	5.6
GEA-1	Gimbal Electronics Assembly-1	Launch	7.1
GEA-2	Gimbal Electronics Assembly-2	Launch	8.6
HST 486	HST 486 Processor	SM3A	6.1
ICU	Instrumentation Control Unit	Launch	11.0
MAT-1	Multiple Access Transponder-1	Launch	9.2
MAT-2	Multiple Access Transponder-2	Launch	9.1
MCU	Mechanisms Control Unit	Launch	8.0
NICMOS	Near Infrared Camera and Multi-Object Spectrometer	SM2	7.0
OCE	Optical Control Electronics	Launch	10.0
OSC-1	Oven-Controlled Crystal Oscillator-1	Launch	5.5
OSC-2	Oven-Controlled Crystal Oscillator-2	Launch	6.4
PCU	Power Control Unit	SM3B	4.3
PDU-1	Power Distribution Unit-1	Launch	7.6
PDU-2	Power Distribution Unit-2	Launch	7.4
PDU-3	Power Distribution Unit-3	Launch	7.6
PDU-4	Power Distribution Unit-4	Launch	7.5
PSEA	Pointing and Safemode Electronics Assembly	Launch	7.8
RSU-1	Rate Sensor Unit-1	Launch and SM4**	3.5
RSU-2	Rate Sensor Unit-2	SM4	3.1
RSU-3	Rate Sensor Unit-3	SM4	3.2
RWAMC-1	Reaction Wheel Assembly Motor Control-1	SM3B	3.6
RWAMC-2	Reaction Wheel Assembly Motor Control-2	Launch	6.4
RWAMC-3	Reaction Wheel Assembly Motor Control-3	Launch	5.7
RWAMC-4	Reaction Wheel Assembly Motor Control-4	Launch	6.2
RWAPE-1	Reaction Wheel Assembly Power Electronics-1	SM3B	5.3
RWAPE-2	Reaction Wheel Assembly Power Electronics-2	Launch	8.3
RWAPE-3	Reaction Wheel Assembly Power Electronics-3	Launch	8.4
RWAPE-4	Reaction Wheel Assembly Power Electronics-4	Launch	8.2
SADE-1	Solar Array Drive Electronics-1	SM1	9.0
SADE-2	Solar Array Drive Electronics-2	SM2	7.0
SI C&DH	Science Instrument Command & Data Handling	SM4	3.3
SSAT-1	S-Band Single Access Transmitter-1	Launch	10.1
SSAT-2	S-Band Single Access Transmitter-2	SM3A	6.4
SSR-1	Solid State Recorder-1	SM2	7.0
SSR-3	Solid State Recorder-3	SM3A	5.8
STIS	Space Telescope Imaging Spectrograph	SM2	6.4
WFC3	Wide Field Camera 3	SM4	2.4

*FGS-2 was taken out of HST during SM3A and re-inserted during SM4

**RSU-1 was taken out of HST during SM1 and re-inserted during SM4

Appendix II

HST parts identified as total dose concerns.

Manufacturer	Part	Generic #	Spacecraft Unit	TID Hardness	Reference
Actel	FPGA	A1280A	SSR	5-10 krad(Si)	[5, 19]
Intersil	Analog multiplexer	IH5108	DIU	10 krad(Si)	[18]
RCA	Quadruple 2 input NAND	4011A	FHST, MAT, RSU	10-20 krad(Si)	[18]
RCA	Quadruple 2 input NAND	CD4011	ESTR	10-20 krad(Si)	[18]
Hughes Aircraft	Microprocessor	1802CD	MAT	5 krad(Si)	[18]
Hughes Aircraft	RAM	1824D	MAT	5 krad(Si)	[18]
Hughes Aircraft	ROM	1832D, 1832CD	MAT	5 krad(Si)	[18]

VI. Acknowledgments

Mike Xapsos thanks Scott Hull and Rich Williams of Goddard Space Flight Center for searching through old HST electronic parts lists to help identify subsystems that contained certain parts. He further thanks Larry Dunham of Goddard Space Flight Center for valuable discussion about the failed LED on the FGS unit.

References

[1] Hubblesite. Available: http://hubblesite.org/hubble_discoveries/
[2] The Hubble Space Telescope. Available: http://asd.gsfc.nasa.gov/archive/hubble/missions/intro.html
[3] "Assessment of Options for Extending the Life of the Hubble Space Telescope", National Research Council, Washington, DC, 2005.
[4] S.J. Gentz et al., "Technical Consultation of the Hubble Space Telescope (HST) System Health Assessment – Analysis of HST Health", NASA/LaRC, Hampton, VA, NASA Engineering and Safety Center Document RP-04-12, Aug. 2004.
[5] J.L. Barth, G.B. Gee and E.G. Stassinopoulos, "Total Ionizing Dose Prediction for the HST-SSR for an 8-Year Mission Duration", NASA/GSFC, Greenbelt, MD, Feb. 1996.
[6] C. Poivey, T. Jordan and K. LaBel, "Radiation Analysis of the Hubble Space Telescope (HST)", NASA/GSFC, Greenbelt, MD, July 2007.
[7] C. Stauffer, C. Poivey, T. Jordan, M. Xapsos and K. LaBel, "Radiation Analysis of the Hubble Space Telescope (HST)", NASA/GSFC, Greenbelt, MD, March 2012.
[8] T. M. Jordan, "An Adjoint Charged Particle Transport Method," IEEE Trans. Nucl. Sci., vol. 23, pp. 1857-1861, Dec. 1976.
[9] D.M. Sawyer and J.I. Vette, "AP-8 Trapped Proton Environment for Solar Maximum and Solar Minimum", NASA/GSFC, Greenbelt, MD, NSSDC/WDC-A-R&S, 76-06, Dec. 1976.
[10] E.J. Daly, J. Lemaire, D. Heynderickx and D.J. Rodgers, "Problems with Models of the Radiation Belts", IEEE Trans. Nucl. Sci., vol. 43, no. 2, pp. 403-414, April 1996.
[11] S.L. Huston, "Space Environments and Effects: Trapped Proton Model", The Boeing Company, Huntington Beach, CA, NAS8-98218, Jan. 2002.
[12] D. Heynderickx, M. Kruglanski, V. Pierrard, J. Lemaire, M.D. Looper and J.B. Blake, "A Low Altitude Trapped Proton Model for Solar Minimum Conditions Based on SAMPEX/PET Data", IEEE Trans. Nucl. Sci., vol. 46, pp. 1475-1480, Dec. 1999.
[13] G. Ginet et al., "The AE9, AP9 and SPM: New Models for Specifying the Trapped Energetic Particle and Space Plasma Environment", Space Sci. Rev., vol. 179, Issue 1-4, pp. 579-615, Nov. 2013.
[14] D. Boscher, A. Sicard-Piet, D. Lazaro, T. Cayton and G. Rolland, "A New Proton Model for Low Altitude High Energy Specification", submitted to IEEE Trans. Nucl. Sci., Dec. 2014 issue.
[15] G.P. Ginet, B.K. Dichter, D.H. Brautigam and D. Madden, "Proton Flux Anisotropy in Low Earth Orbit", IEEE Trans. Nucl. Sci., vol. 54, pp. 1975-1980, Dec. 2007.
[16] Space Weather Prediction Center. Available: http://www.swpc.noaa.gov/SolarCycle/
[17] J.I. Vette, "The AE-8 Trapped Electron Model Environment", NASA/GSFC, Greenbelt, MD, NSSDC/WDC-A-R&S, 91-24, 1991.
[18] G. Lum, "Radiation Reliability Assessment of the Hubble Space Telescope Electronics", Lockheed Martin, Sunnyvale, CA, Technical Memo TM12-97, Feb. 1998.
[19] K. Sahu and S. Kniffin, "Radiation Report on A1280A CQ172B (Actel) (LDC9740), NASA/GSFC, Greenbelt, MD, Oct. 1998.
[20] L. Dunham, private communication, July 2014.
[21] G.P. Summers, E.A. Burke, P. Shapiro, S.R. Messenger and R.J. Walters, "Damage Correlations in Semiconductors Exposed to Gamma, Electron and Proton Radiations", IEEE Trans. Nucl. Sci., vol. 40, pp. 1372-1379, Dec. 1993.